Finite Element Simulation on Uplift Problem of Ground Anchor

T. Okayasu[1], K. Hashiguchi[1], T. Ozaki[2], D. Yajima[1], S. Ozaki[1]

Summary

In this paper the uplift problem of a ground anchor buried in shallow ground is analyzed by the finite element method program incorporating the extended subloading surface model, which falls within the framework of unconventional plasticity and is capable of describing the cyclic loading behavior of materials. The predicted ultimate uplift resistance of an anchor subjected to the monotonic loading and progressive failure of the ground are in agreement with the experimental results. Furthermore, the cyclic deformation behavior, including failure, is predicted realistically for the various levels of cyclic loading amplitude.

Introduction

Various studies on the uplift problem of a ground anchor have been performed from experimental, theoretical of view up to the present. Except for a few experimental results (cf. e.g. [1]), these studies have been confined to analyses only for the uplift resistance of a ground anchor and the progressive failure phenomena of the ground under the monotonic loading condition. However, the ground anchor supporting, for instance, a transmission tower repeatedly has to withstand strong winds and earthquakes; therefore, it is frequently destroyed even if a cyclic force was less than the ultimate uplift resistance. Consequently, in order to design the ground anchor supporting the structures, the proper method to evaluate the uplift resistance to the cyclic loading has to be established.

Amongst numerous existing elastoplastic constitutive models, the *subloading surface model* [2, 3] falling within the framework of the unconventional plasticity which does not use the premise that the interior of yield surface is an elastic domain is capable of realistically describing the smooth elastic-plastic transition. Furthermore, the *extended subloading surface model* [4, 5], in which the similarity-center of the normal yield and the subloading surfaces translate with a plastic deformation, would be capable of describing cyclic loading behavior.

In this paper, the elastoplastic finite element method (FEM) program in which the extended subloading surface model is incorporated is adopted for analyses of the uplift problems of an anchor subjected to not only the monotonic loadings but also the cyclic loadings. First, the ultimate uplift resistance and ground failure phenomena are discussed

1 Department of Bioproduction Environmental Sciences, Graduate School of Kyushu University, Fukuoka 812-8581, JAPAN

2 Kyushu Electric Engineering Consultants Inc., Fukuoka 810-0005, JAPAN

under the monotonic loading condition. Secondly, the cyclic loading phenomena are simulated. Finally, the validity of this program is verified by comparing numerical results with experimental results.

Outline of Extended Subloading Surface

Let it be assumed that stretching $\mathbf{D}$ (the symmetric part of the velocity gradient $\mathbf{L} \equiv \partial \mathbf{v}/\partial \mathbf{x}$; $\mathbf{v}$: velocity) is additively decomposed into elastic stretching $\mathbf{D}^e$ and plastic stretching $\mathbf{D}^p$, i.e.,

$$\mathbf{D} = \mathbf{D}^e + \mathbf{D}^p, \quad \mathbf{D}^e = \mathbf{E}^{-1} \overset{\circ}{\boldsymbol{\sigma}} \tag{1}$$

The fourth-order tensor $\mathbf{E}$ is the elastic modulus, which is given by the Hooke's type. $(\overset{\circ}{})$ is the proper corotational rate.

Now let the *subloading surface* [1, 2] be introduced, which always passes through the current stress $\boldsymbol{\sigma}$ and keeps the similarity to the *normal yield surface*. It is given by

$$f(\overline{\boldsymbol{\sigma}}) = RF(H), \quad \overline{\boldsymbol{\sigma}} \equiv \boldsymbol{\sigma} - \overline{\boldsymbol{\alpha}}, \quad \overline{\boldsymbol{\alpha}} \equiv \mathbf{s} - R(\mathbf{s} - \boldsymbol{\alpha}), \tag{2}$$

where H indicate the isotropic hardening variable. $\overline{\boldsymbol{\alpha}}$ is a conjugate point inside the subloading surface to a reference point inside the normal yield surface. R $(0 \le R \le 1)$ is the ratio of the size of the subloading surface to that of the normal yield surface called the normal-yield ratio. $\mathbf{s}$ is the *similarity-center* of these surfaces. The translation rule of $\boldsymbol{s}$ is assumed as follows

$$\overset{\circ}{\mathbf{s}} = c \left\| \mathbf{D}^p \right\| \frac{\overset{\circ}{\boldsymbol{\sigma}}}{R} + \frac{\overset{\circ}{F}}{F} \mathbf{s} \quad (\overset{\circ}{\boldsymbol{\sigma}} \equiv \boldsymbol{\sigma} - \mathbf{s}), \tag{3}$$

where c (≥ 0) is a material constant and $(\overset{\bullet}{})$ is the material time derivative. $\| \ \|$ stands for the magnitude.

Taking into account the fact that the stress asymptotically approaches the normal yield surface in the plastic loading process, the evolution rule of R is given by

$$\overset{\circ}{R} = U \left\| \mathbf{D}^p \right\| \text{ for } \mathbf{D}^p \ne \mathbf{0}. \tag{4}$$

The function U satisfying the monotonically decreasing function of R is simply given by the concrete form as $U = -u \ln R$, where u (> 0) is a material constant.

The associated flow rule is adopted as

$$\mathbf{D}^p = \lambda \bar{\mathbf{N}} \quad (\|\bar{\mathbf{N}}\| \equiv 1), \tag{5}$$

where $\lambda(>0)$ is the positive proportionality factor and the second-order tensor $\bar{\mathbf{N}}$ is the normalized outward normal to the subloading surface. By substituting Eq. (4) and (5) into the time differentiation of Eq. (2), the positive proportionality factor λ is obtained. The constitutive equation based on this model is given from Eq.(1), (5) and λ as

$$\overset{\circ}{\boldsymbol{\sigma}} = \mathbf{C}^{ep}\mathbf{D} = \left(\mathbf{E} - \frac{\mathbf{E}\bar{\mathbf{N}} \otimes \bar{\mathbf{N}}\mathbf{E}}{\bar{M}_p + \mathrm{tr}(\bar{\mathbf{N}}\mathbf{E}\bar{\mathbf{N}})} \right) \mathbf{D}\,, \tag{6}$$

$$\bar{M}_p = \mathrm{tr}(\bar{\mathbf{N}}\bar{\mathbf{a}}) + \mathrm{tr}(\bar{\mathbf{N}}\bar{\boldsymbol{\sigma}})(F'h/F + U/R)\,,\ \bar{\mathbf{a}} \equiv \overset{\circ}{\bar{\boldsymbol{\alpha}}}/\lambda\,,\ F' \equiv dF/dH\,,\ h \equiv \overset{\circ}{H}/\lambda \tag{7}$$

The loading criterion is given by $\mathbf{D}^p \neq \mathbf{0}$: $\mathrm{tr}(\bar{\mathbf{N}}\mathbf{E}\mathbf{D}) > 0$ and $\mathbf{D}^p = \mathbf{0}$: $\mathrm{tr}(\bar{\mathbf{N}}\mathbf{E}\mathbf{D}) \leq 0$.

Now the following stress function is given for soils specifically as

$$f(\bar{\boldsymbol{\sigma}}) = \bar{p}(1+\bar{\chi}^2)\,,\quad \bar{\boldsymbol{\sigma}}^* = \bar{\boldsymbol{\sigma}} + \bar{p}\mathbf{I}\,,\quad \bar{p} = -\frac{1}{3}\mathrm{tr}\,\bar{\boldsymbol{\sigma}}\,,\quad \bar{\boldsymbol{\eta}} \equiv \frac{\bar{\boldsymbol{\sigma}}^*}{\bar{p}}\,,\quad \bar{c} \equiv \frac{\|\bar{\boldsymbol{\eta}}\|}{\bar{m}}\,, \tag{8}$$

$$\bar{m} = \frac{2\sqrt{6}\sin\phi_{cr}}{3 - \sin\phi_{cr}\sin 3\bar{\theta}_\eta}\,,\quad \sin 3\bar{\theta}_h \equiv -\sqrt{6}\frac{\mathrm{tr}\bar{\boldsymbol{\eta}}^3}{\|\bar{\boldsymbol{\eta}}\|^3}\,,\quad F = F_0 \exp\{H/(\rho-\gamma)\}\,, \tag{9}$$

where ϕ_{cr} is a material constant. F_0 is the initial value of F. ρ and γ are the slopes of the normal consolidation and swelling curve in the $\ln p - \ln v$ (p: pressure, v: volume) space, respectively. H is given by $\overset{\circ}{H} \equiv -D_v^p = -\mathrm{tr}\mathbf{D}$.

Finite Element Method

The rate description of virtual work based on the updated Lagrangian formulation is adopted to predict the uplift problem of the ground anchor as follows

$$\int_v \{\overset{\circ}{\boldsymbol{\sigma}} + (\mathrm{tr}\,\mathbf{D})\boldsymbol{\sigma} - \boldsymbol{\sigma}\mathbf{D} + \mathbf{W}\boldsymbol{\sigma}\} : \delta\mathbf{L}\,dv = \int_s \overset{\circ}{\boldsymbol{\pi}}\delta\mathbf{v}\,ds\,, \tag{10}$$

where $\mathbf{W}$ is the continuum spin (the anti-symmetric part of the velocity gradient $\mathbf{L}$) and $\overset{\circ}{\boldsymbol{\pi}}$ is the nominal traction rate in the current configuration. The letters v and s denote the volume and the area of the body in the current configuration, respectively. $\delta(\,)$ stands for the virtual increment. The present FEM program is developed incorporating the

extended subloading surface model (6) into Eq. (10).

Results and Discussions

Fig. 1 shows the details of the finite element mesh for the analysis, which is considered as the triaxial condition. Ground is discretized into 1512 elements (total 1594 nodes) by the four-noded quadrilateral isoparametric elements. Its bottom is rough, i.e., both the horizontal and vertical displacements are fixed. Both sides are a smooth boundary allowing the vertical displacement. The anchor, radius r, is modeled as the pure elastic solids discretized into 12 elements and is arranged into the right side bottom of the ground. The friction between the anchor and ground is, however, neglected in all analyses. Various levels of prescribed constant load are applied repeatedly on the center bottom of the anchor by the sine curve in the cyclic uplift simulation. The material constants and initial values of the extended subloading surface model are listed in Table 1. The initial stress $\boldsymbol{\sigma}_0$ is given from the overburden pressure, i.e., the vertical and horizontal initial stresses σ_v and σ_h are given by $-\gamma_g h$ (γ_g : unit weight (16.1 kN/m^3), h : ground depth) and $K_0\sigma_v$ (K_0 : coefficient of earth pressure at rest (0.5)), and the initial stress of the similarity center, $\mathbf{s}_0$, is assumed as 1/10 of the initial stress $\boldsymbol{\sigma}_0$.

Fig. 2 shows the uplift load-displacement relation for the monotonic loading condition compared with the experimental data after Sakai and Tanaka [6] and their FEM results. In this analysis, the radius of anchor is fixed 2.5 cm. Then the ground depth is selected as 3 cases 5, 10 and 15cm (ratio of the ground depth to anchor radius, i.e., h/r=2, 4, and 6), respectively. The ultimate uplift stress becomes larger with an increase of h/r and in all experiments the uplift stress decreases gradually after the ultimate stress appeared. The present FEM results totally agree with the experimental results. On the other hand, the FEM results [6] cannot realistically describe the softening behavior.

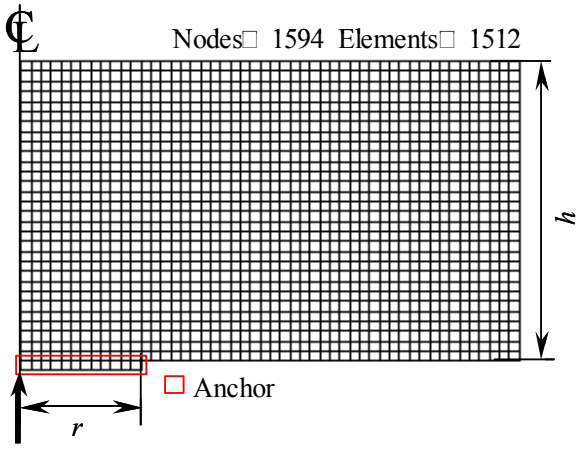

Fig. 1 Finite element mesh.

Table 1 Material constants and initial values.

Item	Value	Item	Value
F_0(kPa)	40.0	ν	0.3
ϕ_{cr} (deg.)	33.0	u	10.0
ρ	0.008	c	10.0
γ	0.0008		

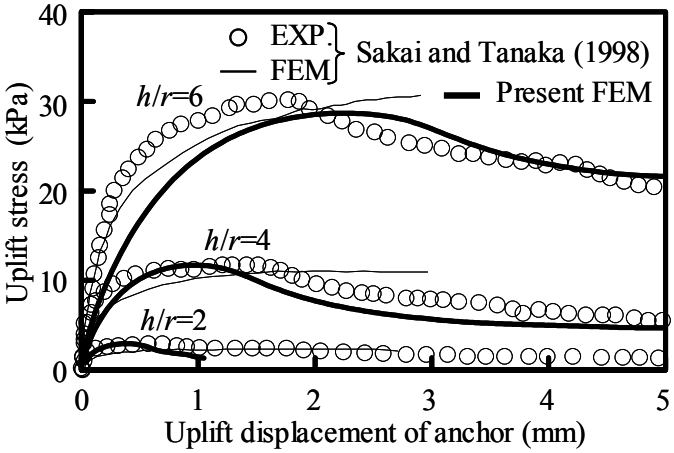

Fig. 2 Comparison of uplift stress-displacement relation.

Fig. 3 shows the relationship between number of loading cycles and uplift displacement of an anchor for various levels of uplift loading. In this analysis, the radius of the anchor and the ground depth are selected as 12 and 30 cm. The amplitudes of cyclic loading are determined as 40, 60, 70, 80 and 90 %, respectively, to the ultimate uplift resistance (572 N) in the monotonic loading simulation. In the case of the big loading amplitude, the uplift displacement increases with the increase of the loading cycle number. It is clearly understood that the ground reaches failure since the increments of the displacement become large. These cyclic loading phenomena are coincident with the experimental data [1]. On the other hand, the modified Cam-clay model (conventional plasticity) can no longer predict the cyclic loading behavior. Fig. 4 shows the deviator strain distributions surrounding the anchor. From this figure the progressive failure due to the development of the localized shear band is exhibited well in the FEM simulation.

Reference

1 Matsuo, M. (1967) "Study on the Uplift Resistance of Footing (I)", *Soil and Foundation*, Vol. 7, No. 4, pp. 1-37.

2 Hashiguchi, K. and Ueno, M. (1977): "Elastoplastic Constitutive Laws of Granular

Materials", *Constitutive Equations of Soils (Proc. 9th Int. Conf. Soil Mech. Found. Eng., Spec. Sess. 9, Tokyo)*, *JSSMFE*, pp.73-82.

3 Hashiguchi, K. (1980): "Constitutive Equations of Elastoplastic Materials with Elastic-Plastic Transition", *J. Appl. Mech. (ASME)*, Vol. 47, pp. 266-272.

4 Hashiguchi, K. (1989): "Subloading Surface Model in Unconventional Plasticity", *Int. J. Solids Struct*., Vol. 25, pp. 917-945.

5 Hashiguchi, K. and Chen, Z.-P. (1998): "Elastoplastic Constitutive Equations of Soils with the Subloading Surface and the Rotational Hardening", *Int. J. Numer. Anal. Meth. Geomech.*. Vol.22, pp.197-227.

6 Sakai, T. and Tanaka, T. (1998): "Scale Effect of a Shallow Circular Anchor in Dense Sand", *Soils and Foundation*, Vol. 38, No. 2, pp. 93-99.

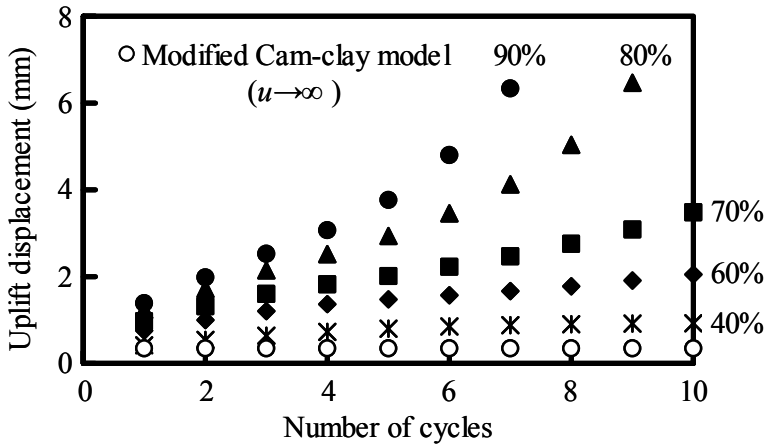

Fig. 3 Relationship between number of loading cycles and uplift displacement of anchor.

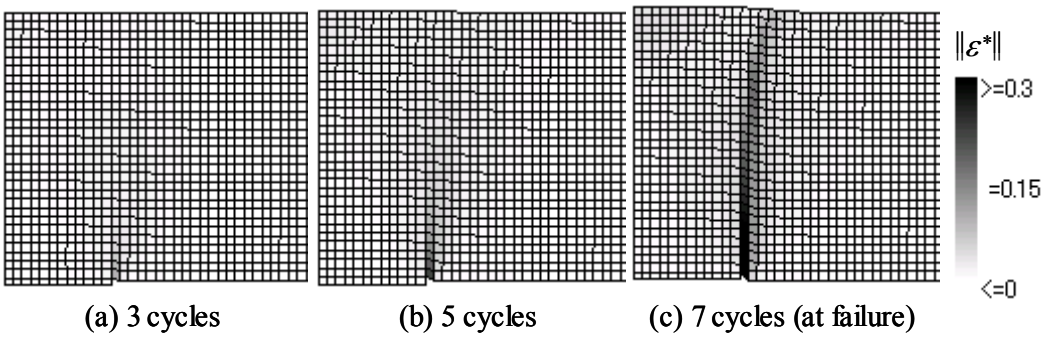

Fig. 4 Deviator strain distributions surrounding anchor (amplitude: 90 %).